Supporting information

Double reactive oxygen species system photoinduced by Cu_8 NCs: synergistic catalysis of phenylacetylene self-coupling reaction

Tingyu Guo, [a] Yapei Yun, [a,*] Tianrong Li, [a] Jun Xia, [a] Jinyan Zhou, [a] Hongting Sheng, [a,*] Manzhou Zhu[a,*]

School of Chemistry & Chemical Engineering, School of Materials Science and Engineering and Anhui Province Key Laboratory of Chemistry for Inorganic/Organic Hybrid Functionalized Materials, Department of Chemistry and Center for Atomic Engineering of Materials, Key Laboratory of Structure and Functional Regulation of Hybrid Materials of the Ministry of Education, Anhui University; Hefei, 230601, China

Materials and Equipment.

Tetraacetonitrile copper hexafluorophosphate ($Cu(CH_3CN)_4PF_6$), cuprous oxide (Cu_2O), carbon disulfide (CS_2), phenylacetylene (C_8H_6), potassium carbonate (K_2CO_3), dichloromethane (CH_2Cl_2), chloroform ($CHCl_3$), sodium borohydride ($NaBH_4$), methanol (CH_3OH), n-hexane (C_6H_{14}), anhydrous ether ($C_4H_{10}O$)

The X-ray photoelectron spectroscopy (XPS) measurements were conducted on ESCALAB 250Xi. Fourier transform infrared (FT-IR) spectra were recorded with Bruker Tensor 27 instrument. UV-vis. spectra were recorded on a Techcomp UV1000 spectrophotometer. The electron paramagnetic resonance (EPR) spectrum was detected by a Bruker ESP-300E spectrometer at 9.8 GHz, X-band, with 100 Hz field modulation. Gas chromatographic (GC) analysis was carried out on an Shimadzu 2010 plus instrument equipped with a flame ionization detector (FID) using high pure N_2 as the carrier gas.

Experimental section

1. Synthesis of the ^{t}BuSCu

ultrasonically disperse 0.5g of cuprous oxide with 60ml of acetonitrile, and slowly add 1ml of ammonia and 1ml of tert-butyl mercaptan to the solution, the solution slowly turns from brick red to grass green, continue to stir for 3-5min, centrifuge, take the clarification solution, and continue to stir for 3h. Centrifuge to obtain a bright yellow precipitate and wash twice with ethanol

2. Synthesis of the Cu_8-1

0.28g of copper tetraacetonitrile hexafluorophosphate was added to 30ml of acetonitrile ultrasonicly dissolved, 0.12g L_1 was dissolved in 30ml of methanol, the L_1 solution was added to the solution of copper tetraacetonitrile hexafluorophosphate, 0.06g sodium borohydride was added after 30min, and the bulk crystals were obtained by diffusion with n-hexane.

3. Synthesis of the Cu_8-2

0.07g of tert-butyl copper sulfide was dissolved in 30ml of chloroform, and 0.07g of L_1 was dissolved in 30ml of methanol, after which it was added to tert-butyl mercaptan and continued to stir for 10 min. The reaction will be volatilized at room temperature in the dark overnight, and dark red block crystals can be obtained after three days.

4. Synthesis of the Cu_8-3

Sonically dissolve 0.07g of copper tert-butyl sulfate in 30ml of chloroform, and 0.07g of L_2 in 30 ml of methanol, then add the solution of copper tert-butyl sulfide and continue to stir for 10min. The reaction solution is volatilized at room temperature, and yellow striped crystals can be obtained after three days.

5. Synthesis of the L_1

Dissolve 1g of carbazole in 10ml of tetrahydrofuran at 0 °C, dissolve 0.7g of potassium tert-butoxide in 5ml of tetrahydrofuran, slowly add potassium tert-butoxide to carbazole tetrahydrofuran solution under stirring, 30 minutes later, add 0.5ml of carbon disulfide dropwise to the reaction system, the system changes from gray-green to bright yellow, and continue to stir at 0 °C for 1h. At the end of the reaction, the solids are washed three times by anhydrous ether.

6. The typical process of phenylene oxidative coupling catalyzed by nanoclusters.

In a 15 mL Shrek reaction tube, phenylacetylene (0.5 mmol), Nanocluster (2 mg) and carbinol (1 mL) was then added and the mixture was magnetically stirred and irradiated by visible-light irradiation (10 W blue LEDs, λ = 400-500 nm, 10 W × 10, Xi 'an Wattecs Experimental Equipment Co., LTD., China) and simultaneously stirred at 500 rpm at room temperature under 1 atm O_2 (balloon) in a Wattecs Parallel Photocatalytic Reactor (WP-TEC-1020HSL, Figure S18). The reaction liquid was concentrated by rotary evaporator and the catalytic reactant was extracted by methanol. The catalytic yield was measured by Shimadzu GC Plus 2010. The remaining solid clusters were washed three times with methanol and were ready for further use.

7. Electron Paramagnetic Resonance (EPR).

The signals of free radicals were obtained on electron paramagnetic resonance (EPR) spectrometer (Bruker EMXplus) using the 5,5-dimethyl-1-pyrroline N-oxide (DMPO) and 2,2,6,6-tetramethylpiperidine (TEMP) as the trapping agent. Specifically, for the test of $O_2^{\cdot-}$, 2 mg catalysts were dispersed in DMPO/methanol solution. The signals were collected under dark and light irradiation (λ > 400 nm). For the test of •OH, 2 mg catalysts were dispersed in DMPO/H_2O solution. For the test of $^1O_2$, 2 mg catalysts were dispersed in TEMP/H_2O solution.

8. Calculation of active oxygen utilization

Under the same conditions, the signal of reactive oxygen species was measured by EPR to ensure that the quality of the three clusters added was the same, and the signal of reactive oxygen species after light was recorded, and then the amount of phenylacetylene of the same substance was added to record the signal of reactive oxygen species after the addition of phenylacetylene. By calculating the difference between the two signals, it is regarded as the signal change caused by the interaction of phenylacetylene with clusters, and the reduced value is divided by the initial value to obtain the utilization rate.

Figure and table

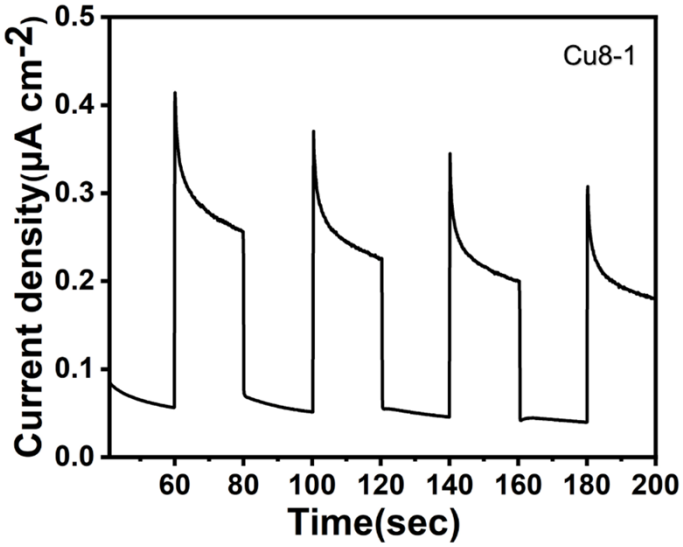

Figure S1: Transient photocurrent density curves of Cu_8-1

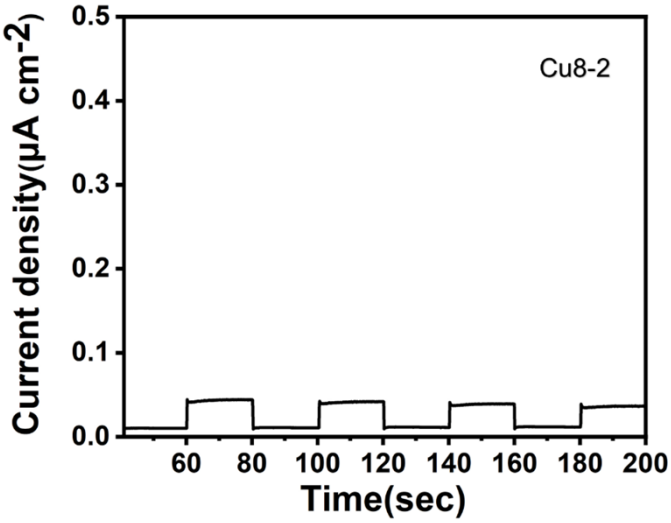

Figure S2: Transient photocurrent density curves of Cu_8-2

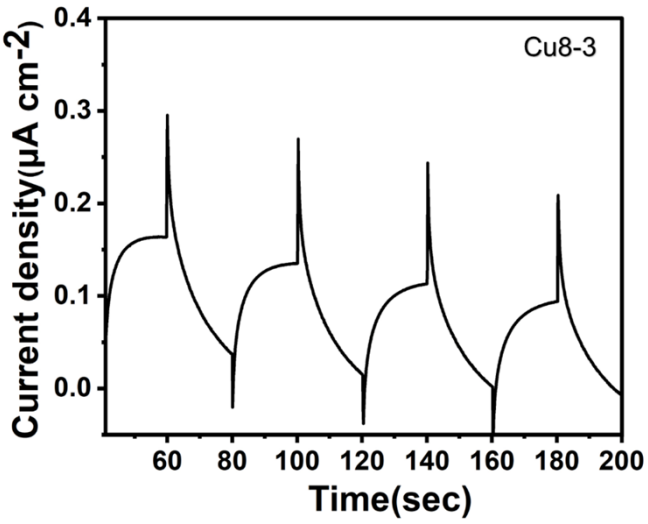

Figure S3: Transient photocurrent density curves of Cu_8-3

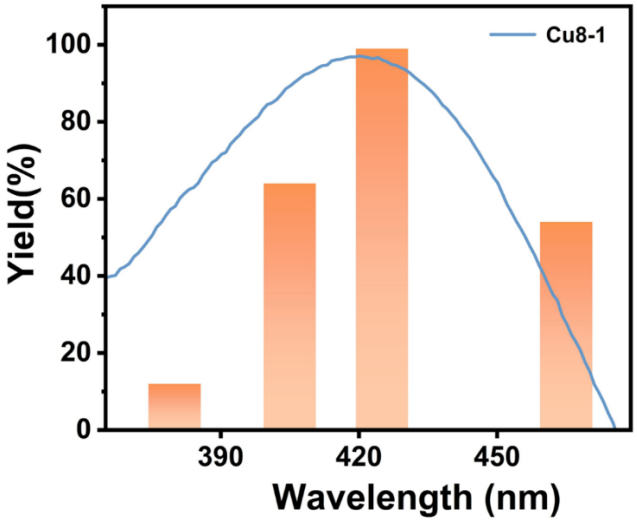

Figure S4: Yield curves of Cu_8-1 catalyst at different wavelengths

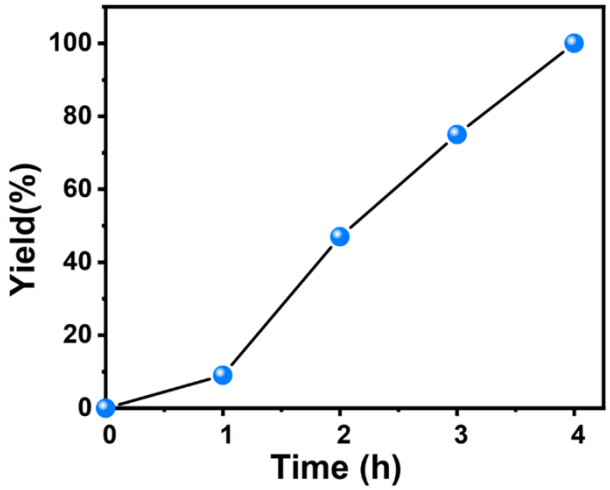

Figure S5: Yield curves of Cu_8-1 catalyst as a function of time

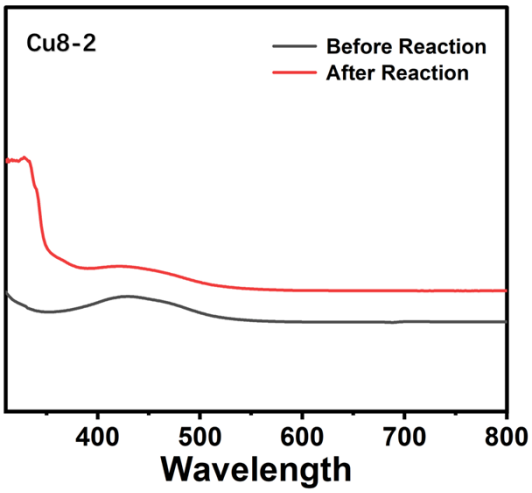

Figure S6: Ultraviolet absorption curves of Cu_8-2 catalyst before and after reaction

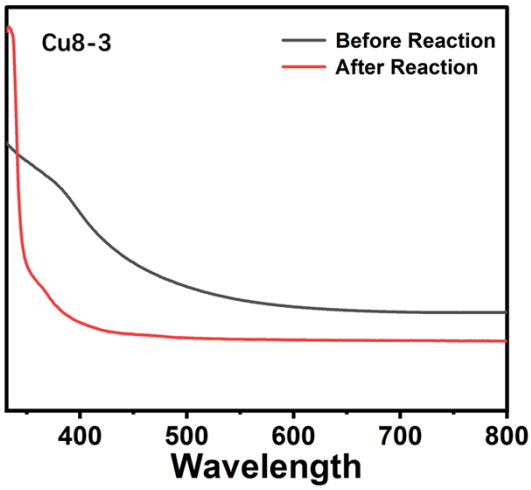

Figure S7: Ultraviolet absorption curves of Cu_8-3 catalyst before and after reaction

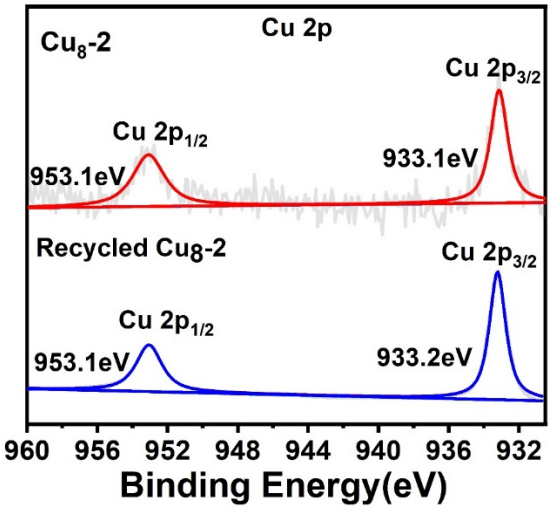

Figure S8: XPS curves before and after Cu_8-2 catalyst reaction

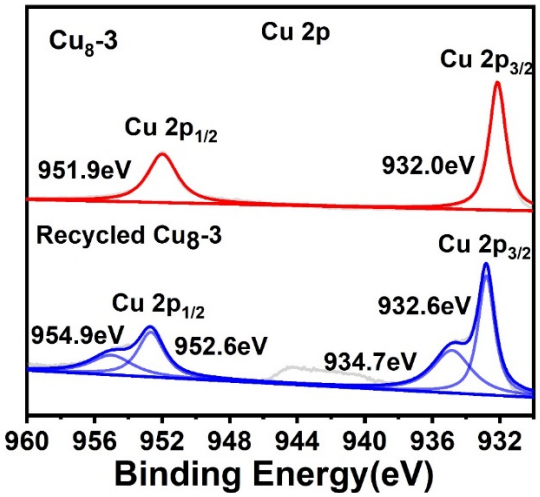

Figure S9: XPS curves before and after Cu_8-3 catalyst reaction

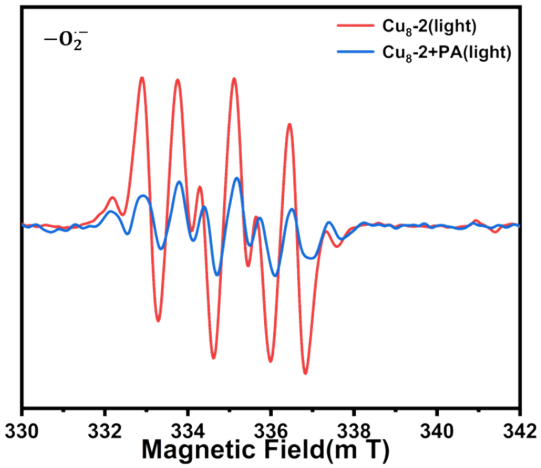

Figure S10: O·⟝ **2** signals of Cu_8-2 after light and Cu_8-2 after addition of phenylacetylene

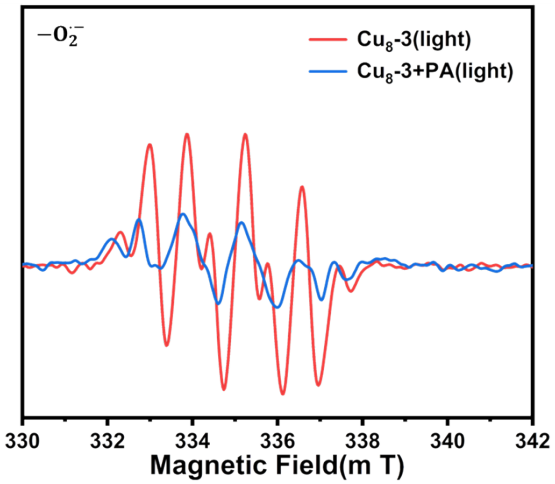

Figure S11: O·⟝ **2** signals of Cu_8-3 after light and Cu_8-3 after addition of phenylacetylene

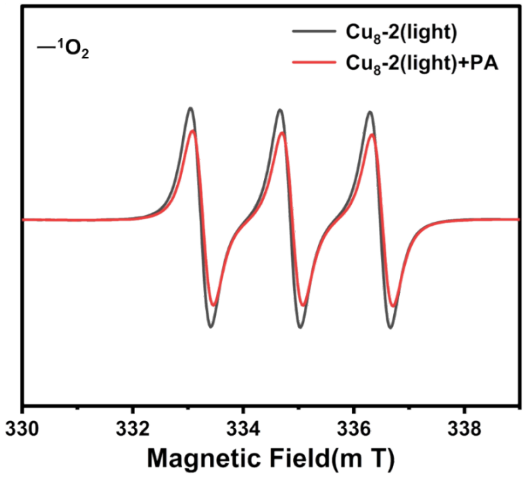

Figure S12: $^1O_2$ signals of Cu_8-2 after light and Cu_8-2 after addition of phenylacetylene

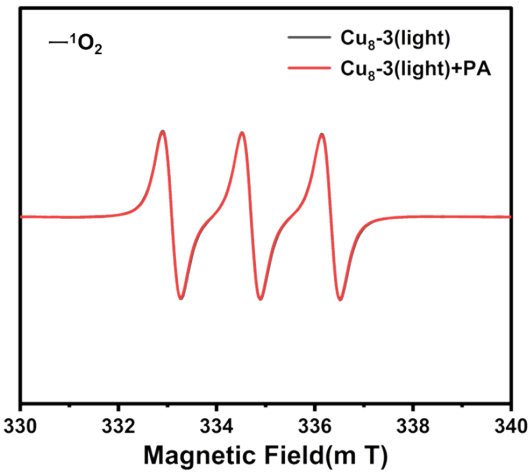

Figure S13: $^1O_2$ signals of Cu_8-3 after light and Cu_8-3 after addition of phenylacetylene

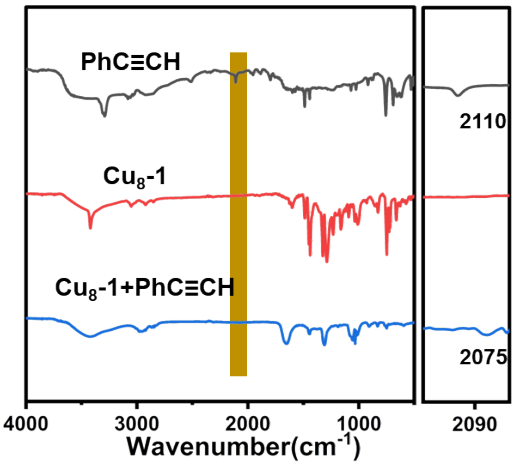

Figure S14: FT-IR spectrum of Cu_8-1, Phenylacetylene and Cu_8-1 mixed with Phenylacetylene

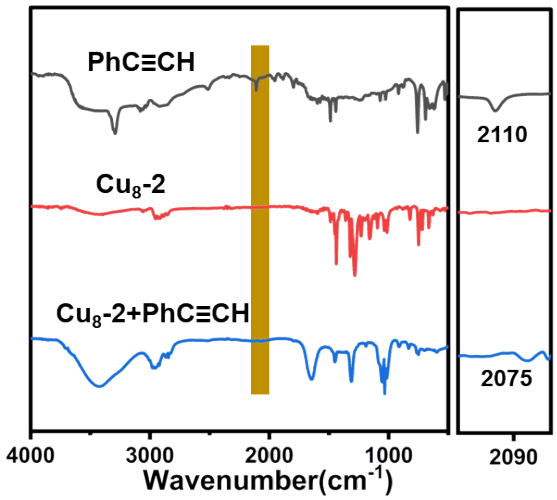

Figure S15: FT-IR spectrum of Cu_8-2, Phenylacetylene and Cu_8-2mixed with Phenylacetylene

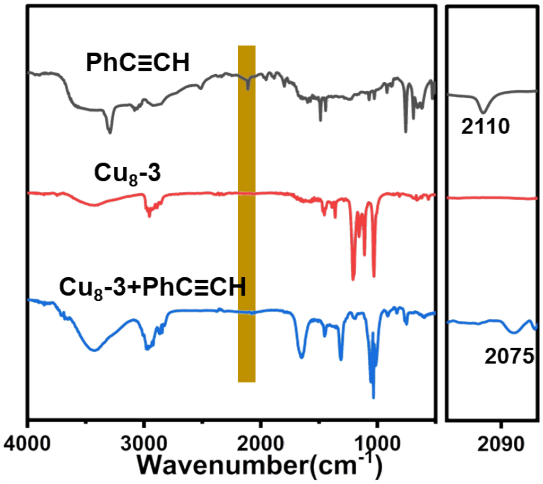

Figure S16: FT-IR spectrum of Cu_8-3, Phenylacetylene and Cu_8-3 mixed with Phenylacetylene

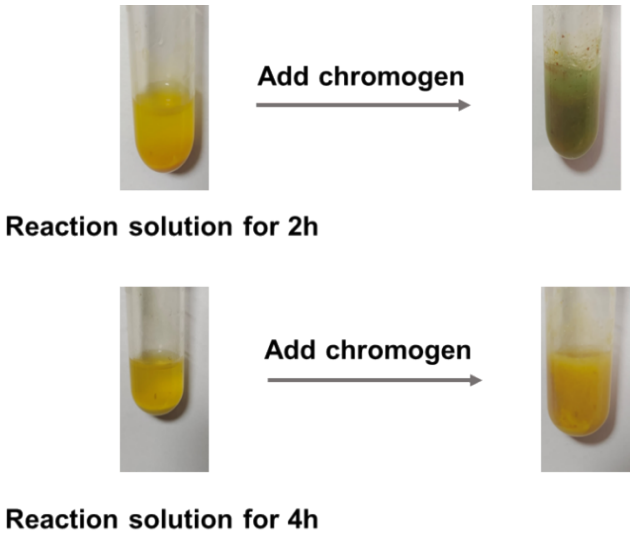

Figure S17: Color development of H_2O_2

Figure S18: The picture of photocatalytic reactor. The photocatalytic reaction was performed on WATTCAS Parallel Photocatalytic Reactor (WP-TEC-LC) with 10W COB LED.

Table S1 Effect of different catalysts on the activity of photocatalytic phenylene coupling reaction

Cat.	Condition	TON	Ref.
Cu−Cu_2O−C	1 atm CO_2, rt, 20h, white light	3.0	1
CuSA/ZIF	rt,425nm,100min	580.6	2
Cu/C_3N_4	rt., O_2, 6h	9.9	3
CuI	O_2, rt, blue light,7h	19.6	4
Cu/MnO_x	25℃, air, 3h	15.8	5
Cu_1/NC-800	100 °C, air, 18 h	26.1	6
Cu_8-1	2mg,4h, rt,425nm	524.0	This work

References.

1. J. Cai, Y. Li, M. Zhang and Z. Li, *Inorg. Chem.*, 2019, **58**, 7997-8002.
2. Y. Yun, H. Zeng, L. Li, H. Li, , *Adv. Mater.*, 2023, **35**, e2209561.
3. H. Xu, K. Wu, J. Tian, L. Zhu and X. Yao, *Green Chem.*, 2018, **20**, 793-797.
4. Sagadevan, V. P. Charpe and K. C. Hwang, *Catal. Sci. Technol.*, 2016, **6**, 7688-7692.
5. Toledo, I. Funes-Ardoiz, F. Maseras and A. C. Albéniz, *ACS Catal.*, 2018, **8**, 7495-7506.
6. P. Ren, Q. Li, T. Song and Y. Yang, *ACS Appl. Mater. Interfaces*, 2020, **12**, 27210-27218.